

## References and Notes

1. T. I. Lee *et al.*, *Science* **298**, 799 (2002).
2. T. Ideker *et al.*, *Science* **292**, 929 (2001).
3. A. Arkin, P. D. Shen, J. Ross, *Science* **277**, 1275 (1997).
4. S. Maslov, K. Sneppen, *Science* **296**, 910 (2002).
5. E. Ravasz, A. L. Somera, D. A. Mongru, Z. N. Oltvai, A.-L. Barabási, *Science* **297**, 1551 (2002).
6. J. S. Edwards, B. O. Palsson, *Proc. Natl. Acad. Sci. U.S.A.* **97**, 5528 (2000).
7. E. H. Davidson *et al.*, *Science* **295**, 1669 (2002).
8. S. S. Shen-Orr, R. Milo, S. Mangan, U. Alon, *Nature Genet.* **31**, 64 (2002).
9. U. S. Bhalla, R. Iyengar, *Science* **283**, 381 (1999).
10. S. Liang, S. Fuhrman, R. Somogyi, *Proc. Pac. Symp. Biocomp.* **3**, 18 (1998).
11. P. D'Haeseleer, X. Wen, S. Fuhrman, R. Somogyi, *Proc. Pac. Symp. Biocomp.* **4**, 41 (1999).
12. E. P. van Someren, L. F. A. Wessels, M. J. T. Reinders, E. Backer, *Proceedings of the 2nd International Conference on Systems Biology* (Caltech, Pasadena, CA, 2001), pp. 222–230.
13. L. Ljung, *System Identification: Theory for the User* (Prentice Hall, Upper Saddle River, NJ, 1999).
14. H. H. McAdams, A. Arkin, *Annu. Rev. Biophys. Biomol. Struct.* **27**, 199 (1998).
15. H. de Jong, *J. Comput. Biol.* **9**, 67 (2002).
16. A. de la Fuente, P. Brazhnik, P. Mendes, *Trends Genet.* **18**, 395 (2002).
17. D. Thieffry, A. M. Huerta, E. Pérez-Rueda, J. Collado-Vides, *Bioessays* **20**, 433 (1998).
18. J. Tegner, M. K. Yeung, J. Hasty, J. J. Collins, *Proc. Natl. Acad. Sci. U.S.A.* **100**, 5944 (2003).
19. H. Jeong, S. P. Mason, A.-L. Barabási, Z. N. Oltvai, *Nature* **411**, 41 (2001).
20. D. Montgomery, E. A. Peck, G. G. Vining, *Introduction to Linear Regression Analysis* (Wiley, New York, 2001).
21. J. Courcelle, A. Khodursky, B. Peter, P. O. Brown, P. C. Hanawalt, *Genetics* **158**, 41 (2001).
22. G. C. Walker, in *Escherichia coli and Salmonella: Cellular and Molecular Biology* (American Society for Microbiology, Washington, DC, ed. 2, 1996), pp. 1400–1416.
23. W. H. Koch, R. Woodgate, in *DNA Damage and Repair*, vol. 1, *DNA Repair in Prokaryotes and Lower Eukaryotes* (Humana, Totowa, NJ, 1998), pp. 107–134.
24. A. R. Fernández de Henestrosa *et al.*, *Mol. Microbiol.* **35**, 1560 (2000).
25. P. D. Karp *et al.*, *Nucleic Acids Res.* **30**, 56 (2002).
26. K. Lewis, *Microbiol. Mol. Biol. Rev.* **64**, 503 (2000).
27. Materials, methods, and supporting data are available as supporting material on Science Online.
28. C. Ding, C. R. Cantor, *Proc. Natl. Acad. Sci. U.S.A.* **100**, 3059 (2003).
29. We thank J. Tegner for his insights on this work, H. Schaeffer for his guidance on qPCR, and the Department of Biology at Boston University for access to their qPCR facility. This work was supported by the Defense Advanced Research Projects Agency, NSF, the Office of Naval Research, the Human Frontiers Science Program, and the Telethon Institute of Genetics and Medicine.

## Supporting Online Material

www.sciencemag.org/cgi/content/full/301/5629/102/DC1

Materials and Methods

SOM Text

Figs. S1 to S5

Tables S1 to S8

References

24 December 2002; accepted 3 June 2003

## Intracellular Bacterial Biofilm-Like Pods in Urinary Tract Infections

Gregory G. Anderson,<sup>1\*</sup> Joseph J. Palermo,<sup>1\*</sup> Joel D. Schilling,<sup>1</sup> Robyn Roth,<sup>2</sup> John Heuser,<sup>2</sup> Scott J. Hultgren<sup>1†</sup>

*Escherichia coli* entry into the bladder is met with potent innate defenses, including neutrophil influx and epithelial exfoliation. Bacterial subversion of innate responses involves invasion into bladder superficial cells. We discovered that the intracellular bacteria matured into biofilms, creating pod-like bulges on the bladder surface. Pods contained bacteria encased in a polysaccharide-rich matrix surrounded by a protective shell of uroplakin. Within the biofilm, bacterial structures interacted extensively with the surrounding matrix, and biofilm associated factors had regional variation in expression. The discovery of intracellular biofilm-like pods explains how bladder infections can persist in the face of robust host defenses.

Urinary tract infections (UTIs) result in \$1.6 billion in medical expenditures in the United States each year (1), with uropathogenic strains of *Escherichia coli* (UPEC) accounting for 70 to 95% of all UTIs (2). With the advance of multi-drug-resistant UPEC (3), it is important to determine the pathogenic mechanisms of UPEC. In animal models, UPEC pathogenesis initiates with bacterial binding of superficial bladder epithelial cells via the adhesin FimH at the tips of bacterially expressed type 1 pili (4). Initial colonization events activate inflammatory and apoptotic cascades in the epithelium, which is normally inert and only turns over every 6 to 12 months (5). Bladder epithelial cells respond to invading bacteria in part by recognizing bacterial lipopolysaccharide (LPS) via the Toll-like recep-

tor 4 (TLR-4)–CD14 pathway, which results in strong neutrophil influx into the bladder (6). In addition, FimH-mediated interactions with the bladder epithelium stimulate exfoliation of superficial epithelial cells, causing many of the pathogens to be shed into the urine. Genetic programs are activated that lead to differentiation and proliferation of the underlying transitional cells in an effort to renew the exfoliated superficial epithelium (7). Despite the robust inflammatory response and epithelial exfoliation, UPEC are able to maintain high titers in the bladder for several days (8–13).

A bacterial mechanism of FimH-mediated invasion into the superficial cells apparently allows evasion of these innate defenses (9); subsequent replication as disorganized bacterial clusters inside superficial cells leads to high bacterial titers in the bladder. Bacteria in these intracellular niches [which we termed “bacterial factories” (9)] create a chronic quiescent reservoir in the bladder, which can persist undetected for several months without bacteria shedding in the urine. These bacteria are completely resistant to 3- and 10-day courses of antibiotics (9, 14).

Thus, in addition to the intestine and vagina as reservoirs for UPEC, the bladder itself may serve as the source for recurrent cystitis and asymptomatic bacteriuria seen in a large proportion of women with UTIs (9, 14, 15).

To define bacterial-specific effects on UTI progression, we studied acute UTIs initiated by clinically isolated UPEC or laboratory (K-12) strains in TLR-4 mutant C3H/HeJ mice, which lack an intact innate immune response (16, 17). C3H/HeJ mice were inoculated with UPEC strain UTI89 (9) or type 1-piliated K-12 strain MG1655 (18), and numbers of colony-forming units (CFU) were determined in bladders at early time points after inoculation (fig. S1) (10, 19). While UTI89 levels increased nearly two orders of magnitude over 24 hours to about  $6 \times 10^6$  CFU per bladder, MG1655 levels decreased over this time period to  $10^3$  CFU per bladder.

To investigate the increase in UPEC bacterial load at 24 hours, we performed scanning electron microscopy (SEM) (8, 10) of infected C3H/HeJ mouse bladders, which revealed numerous, large protrusions, or pods, on the surface of bladders infected with UPEC strain UTI89 (Fig. 1, A to C) (fig. S2). This was a rare event with the K-12 strain of *E. coli*, MG1655, because pods were not detected at this time point (Fig. 1D). In contrast, other clinical isolates such as UPEC strain NU14 (9, 10) also elicited abundant pod formation. SEM and hematoxylin and eosin (H&E) staining of the pods revealed that bacterial replication resulted in large bacterial colonies that extended above the luminal surface (Fig. 1E). Video microscopy revealed that the previously described bacterial factories undergo a maturation process (20), whereby the loose collections of UPEC rods converted into a uniform coccoid morphology. This process was coupled with the organization of the bacteria into tightly packed biofilm-like pod structures (Fig. 1E) (20). Mutations in *fimH* completely abolish this pathogenic cascade (10).

<sup>1</sup>Department of Molecular Microbiology, <sup>2</sup>Department of Cell Biology and Physiology, Washington University School of Medicine, 660 South Euclid Avenue, St. Louis, MO 63110, USA.

\*These authors contributed equally to this work.

†To whom correspondence should be addressed. E-mail: hultgren@borcim.wustl.edu

## REPORTS

Bladders from the corresponding TLR-4 wild-type C3H/HeN mice also contained pods, which were shown by H&E stains and SEM to be identical to those in C3H/HeJ mice (Fig. 1F). However, about one-tenth as many pods were seen in C3H/HeN mice, probably because of the presence of an intact immune system and correspondingly increased inflammation (11). Pods were not visualized in previous UPEC studies using the C57/Bl6 mouse strain, possibly because of a more robust exfoliation response in that mouse strain (9, 10). These findings underscore the effect of genetic variability present in different host populations and the importance of strategies for pathogen persistence despite differing host defenses.

In contrast with the ruffled appearance of normal bladder epithelium, the luminal shell of each pod was smooth (Fig. 1, A and B). We visualized whole-mounted bladders infected with UT189 expressing green fluorescent protein (GFP) (21) and stained with antibodies to uroplakin, which is an integral membrane protein that forms an organized crystalline array covering the luminal surface of the bladder epithelium (22–24). A Z-section series obtained by confocal laser microscopy revealed large accumulations of GFP-expressing bacteria underneath the uroplakin coating (Fig. 1G). Although the pod shell contains uroplakin, this finding does not exclude the possibility that the shell is somehow modified by bacterial contributions.

The pod interior, apparent by SEM through cracks in the shell, showed bacteria embedded in a fibrous matrix (Fig. 1, B and C). Transmission electron microscopy (TEM) showed that the bacteria were not confined to a membrane-bound compartment; rather, they were located free in the host cell cytoplasm, within a matrix of vesicles, fibers, and membrane fragments (Fig. 2, A and B). Moreover, an electron-lucent halo surrounded each bacterium, separating the bacteria from each other and from epithelial cell contents (Fig. 2, A and B).

To investigate the cellular basis of the halos and to gain a more detailed understanding of the pod organization, we performed freeze-fracture electron microscopy, a technique useful for preserving ultrastructural details and relationships disrupted by other microscopic methods (10, 25). High-resolution microscopy revealed that every bacterium was compartmentalized within the matrix and interacted extensively with the matrix via abundantly expressed fibers (Fig. 2, C and D). The distal end of virtually every fiber was buried in the matrix at a uniform distance from the bacterial outer membrane (Fig. 2E). Together, the matrix and bacterial fibers intertwined in a network that seemed to provide a scaffold of support for each bacterium (Fig. 2, C and D). Occasionally, fibers from adjacent bacteria interacted (26); however, most bacteria appeared insulated from other microbes.

The highly organized nature of the bacteria embedded in a cytoplasmic matrix sug-

gested that UPEC form a biofilm inside bladder epithelial cells. Biofilms have been found in both environmental and in vivo systems but have never been described within a eukaryotic cell (27, 28). Virtually all biofilms involve aggregated bacteria attached to a surface and encased in a polysaccharide matrix, within which differential gene expression leads to distinct bacterial subpopulations. During infection, the biofilm milieu renders bacteria resistant to antibiotics and host defenses, making the infection difficult to treat and leading to recurrent symptoms (27). Several factors expressed by *E. coli* are involved in biofilm formation, including type 1 pili and antigen 43, an autotransporter protein promoting autoaggregation (29, 30). Immu-

nofluorescent staining of thin bladder sections for type 1 pili showed strong but heterogeneous labeling in the pod (Fig. 3A), which suggests that many but not all of the bacteria were expressing type 1 pili. Similarly, we found strong regional expression of antigen 43 (Fig. 3B) (31). Given that UPEC contain as many as nine different chaperone/usher pathways to assemble pili (32), many other pilus fibers may be regionally expressed in the pod. Pods also exhibited a strong, uniform distribution of polysaccharides identified with periodic acid–Schiff (PAS) reagent, a previously published method for detecting biofilm polysaccharides in host tissues (Fig. 3C) (33). Thus, some of the fibrous-looking material surrounding the bacteria may actu-

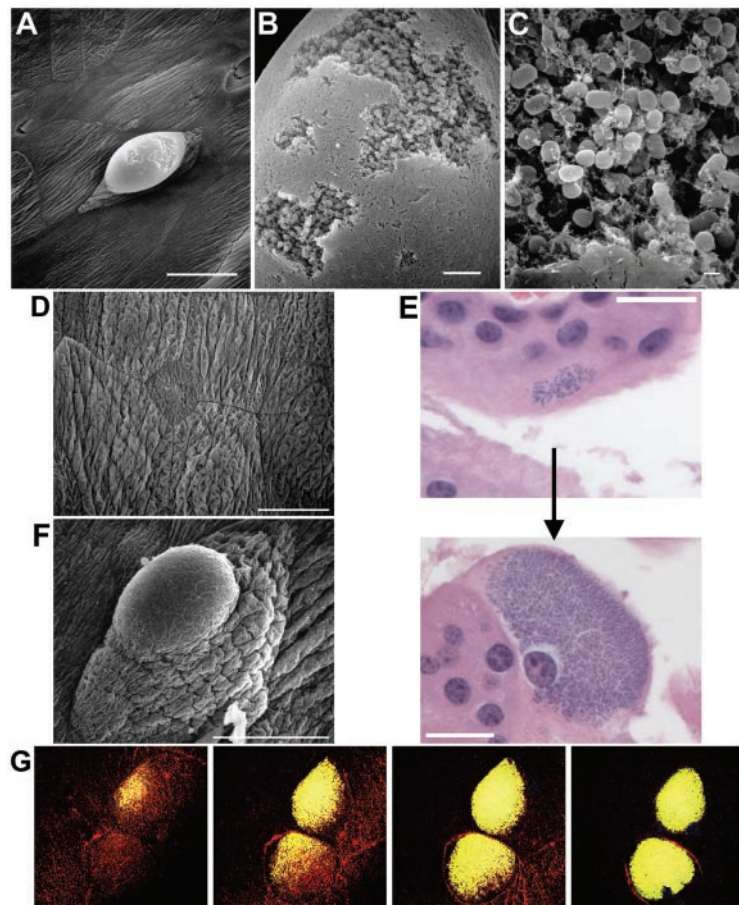


**Fig. 1.** Intracellular bacterial communities extend like pods into the bladder lumen. Infected bladders were bisected, fixed, and visualized by either SEM or light microscopy (H&E staining). (A to C) SEM images of a pod on the surface of a C3H/HeJ mouse bladder infected with UT189 for 24 hours show large intracellular communities of bacteria inside pods. Scale bars, 50  $\mu\text{m}$  (A), 5  $\mu\text{m}$  (B), 0.5  $\mu\text{m}$  (C). (D) SEM revealed no pods in C3H/HeJ bladders infected with MG1655. Scale bar, 50  $\mu\text{m}$ . (E) H&E-stained sections of UT189-infected C3H/HeJ mouse bladders show a bacterial factory 6 hours after inoculation (top panel) and a pod 24 hours after inoculation (bottom panel). Bacteria in the pod were densely packed, shorter, and completely filled the host cell. Video microscopy has shown that bacterial factories mature into pods (20). Scale bars, 20  $\mu\text{m}$ . (F) Pods were evident in wild-type C3H/HeN bladders infected with UT189. Scale bar, 50  $\mu\text{m}$ . (G) Confocal Z-section series from whole-mounted bladder infected with UT189 expressing green fluorescent protein from the plasmid pcomGFP (19) and stained with antibody to uroplakin (primary antibody) and tetramethyl rhodamine isothiocyanate–labeled secondary antibody, showing uroplakin coating the surface of pods. The series depicts the luminal surface on the left and progresses through the epithelium toward the right. Optical section thickness, 1  $\mu\text{m}$ . All images are representative of the entire sample surface and are from bladders harvested 24 hours after inoculation, unless otherwise indicated.

ally represent a glycocalyx. The presence of a polysaccharide matrix surrounding differentiated subpopulations of bacteria is consistent with the formation of a biofilm.

Entry of *E. coli* into the urinary tract is not well understood, although sexual intercourse is the most clearly defined predisposing factor (2). Presumably, a small number of *E. coli* from the vaginal or enteric flora are introduced into the bladder during an average incident, and it seems plausible that in most cases the innate defenses in the bladder would be able to prevent infection. However, with more than 8 million cases of UTI annually (1), UPEC clearly possess mechanisms to overcome these defenses and establish a foothold in the bladder. A recent genomic analysis of UPEC strain CFT073 identified numerous dif-

ferences between this pathogenic isolate and K-12 strain MG1655 (32). The deficiency of pods at 24 hours in MG1655-infected mice suggests that alterations in the UTI89 genome have conferred the ability to subvert host defenses through pod formation and persistence. The impermeable uroplakin shell of the pod would also provide an environment sequestering the bacteria from antibiotics concentrated in the urine as well as from host inflammatory responses, thus allowing the bacteria to proliferate, differentiate, and survive.

Pods represent a previously undescribed intracellular microbial community in which bacterial differentiation results in subpopulations with possible survival advantages. We previously described a bacterial differentiation whereby intra-

cellular UPEC flux from host cells, often in a filamentous state, prior to clearance from the host (9). Because pod formation correlated with increased bacterial titers, pods may facilitate an efficient spread of the organism during fluxing, thus allowing enough bacteria to survive host defenses and reinvade the bladder epithelium to form a persistent reservoir (20). Intracellular biofilms may be vital for UTI progression, and their identification establishes a new paradigm in our understanding of acute and recurrent UTIs. Similar structures may also be involved in the pathogenesis of other chronic or recurrent infections as a common survival strategy for invasive microorganisms.

References and Notes

1. B. Foxman, *Am. J. Med.* **113** (suppl. 1A), 5S (2002).
2. T. M. Hooton, W. E. Stamm, *Infect. Dis. Clin. North Am.* **11**, 551 (1997).
3. A. R. Manges et al., *N. Engl. J. Med.* **345**, 1007 (2001).
4. M. A. Mulvey, J. D. Schilling, J. J. Martinez, S. J. Hultgren, *Proc. Natl. Acad. Sci. U.S.A.* **97**, 8829 (2000).
5. R. M. Hicks, *Biol. Rev. Camb. Philos. Soc.* **50**, 215 (1975).
6. J. D. Schilling, M. A. Mulvey, C. D. Vincent, R. G. Lorenz, S. J. Hultgren, *J. Immunol.* **166**, 1148 (2001).
7. I. U. Mysorekar, M. A. Mulvey, S. J. Hultgren, J. I. Gordon, *J. Biol. Chem.* **277**, 7412 (2002).
8. J. J. Martinez, M. A. Mulvey, J. D. Schilling, J. S. Pinkner, S. J. Hultgren, *EMBO J.* **19**, 2803 (2000).
9. M. A. Mulvey, J. D. Schilling, S. J. Hultgren, *Infect. Immun.* **69**, 4572 (2001).
10. M. A. Mulvey et al., *Science* **282**, 1494 (1998).
11. M. Haraoka et al., *J. Infect. Dis.* **180**, 1220 (1999).
12. G. Otto, J. Braconier, A. Andreasson, C. Svanborg, *J. Infect. Dis.* **179**, 172 (1999).
13. L. E. Olsson, M. A. Wheeler, W. C. Sessa, R. M. Weiss, *J. Pharmacol. Exp. Ther.* **284**, 1203 (1998).
14. J. D. Schilling, R. G. Lorenz, S. J. Hultgren, *Infect. Immun.* **70**, 7042 (2002).
15. B. Foxman, *Am. J. Public Health* **80**, 331 (1990).
16. J. D. Schilling, S. M. Martin, C. S. Hung, R. G. Lorenz, S. J. Hultgren, *Proc. Natl. Acad. Sci. U.S.A.* **100**, 4203 (2003).
17. A. Poltorak et al., *Science* **282**, 2085 (1998).
18. F. R. Blattner et al., *Science* **277**, 1453 (1997).
19. See supporting data on Science Online.
20. S. Justice et al., in preparation.
21. B. P. Cormack, R. H. Valdivia, S. Falkow, *Gene* **173**, 33 (1996).
22. X. R. Wu, M. Manabe, J. Yu, T. T. Sun, *J. Biol. Chem.* **265**, 19170 (1990).
23. S. A. Lewis, *Am. J. Physiol. Renal Physiol.* **278**, F867 (2000).
24. P. Hu et al., *Am. J. Physiol. Renal Physiol.* **283**, F1200 (2002).
25. J. E. Heuser, *J. Muscle Res. Cell Motil.* **8**, 303 (1987).
26. G. G. Anderson et al., data not shown.
27. R. M. Donlan, J. W. Costerton, *Clin. Microbiol. Rev.* **15**, 167 (2002).
28. W. M. Dunne Jr., *Clin. Microbiol. Rev.* **15**, 155 (2002).
29. L. A. Pratt, R. Kolter, *Mol. Microbiol.* **30**, 285 (1998).
30. P. N. Danese, L. A. Pratt, S. L. Dove, R. Kolter, *Mol. Microbiol.* **37**, 424 (2000).
31. P. Owen, P. Caffrey, L. G. Josefsson, *J. Bacteriol.* **169**, 3770 (1987).
32. R. A. Welch et al., *Proc. Natl. Acad. Sci. U.S.A.* **99**, 17020 (2002).
33. T. P. Fulcher et al., *Ophthalmology* **108**, 1088 (2001).
34. We thank M. Veith and W. Beatty for assistance with scanning and transmission microscopy; P. Owen, T. T. Sun, and MedImmune Inc. for their kind donations of antibodies; and K. Dodson and M. Chapman for helpful comments. Supported by NIH grants AI29549, DK51406, and AI48689, and by ORWH SCOR grant DK64540 in partnership with DHHS, NIDDK, and the FDA.

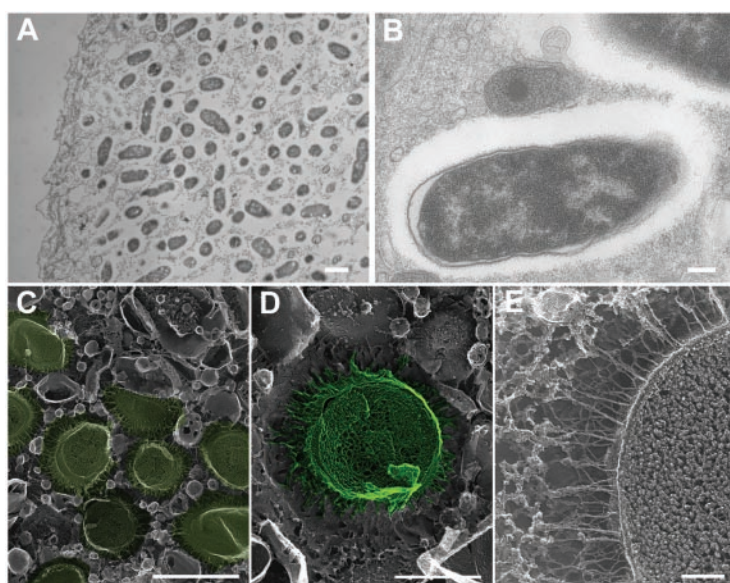


**Fig. 2.** Bacteria in pods are embedded in a matrix in the host cell cytoplasm. (A and B) TEM images of the pod interior show bacteria surrounded by an electron-lucent halo. However, the bacteria appear to be located in the host cell cytoplasm and not in membrane-bound vacuoles. Scale bars, 1 μm (A), 0.2 μm (B). (C to E) High-resolution freeze-fracture images of the pod interior depict an organized structure of the bacteria, with numerous fibers interacting with the surrounding matrix. Scale bars, 1 μm (C), 0.5 μm (D), 0.1 μm (E). In (C) and (D), bacteria were pseudo-colored green. All images were obtained from C3H/HeJ mouse bladder 24 hours after inoculation with UTI89.

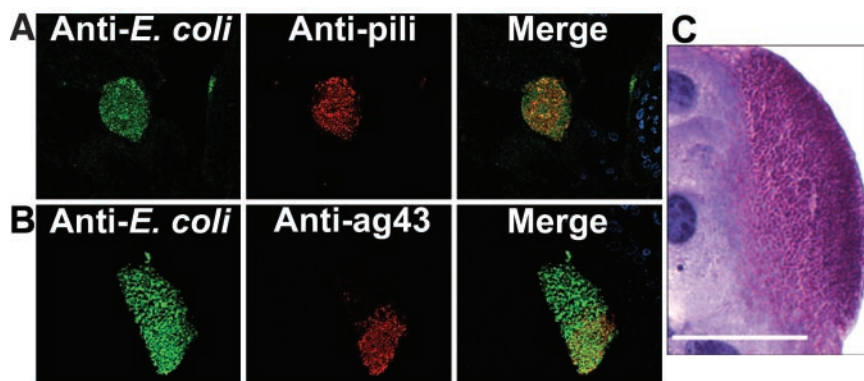


**Fig. 3.** Bacteria in pods express type 1 pili, antigen 43, and polysaccharides. Pods were immunostained for type 1 pili (A) and antigen 43 (B) in combination with antibodies to *E. coli*, and their images were merged (right panels). Yellow indicates antibody colocalization. (C) PAS-stained thin bladder section shows a polysaccharide-filled pod. Scale bar, 20 μm. The regional expression of type 1 pili and antigen 43 within a polysaccharide matrix suggests that pods form a biofilm inside host bladder cells.

**Supporting Online Material**  
[www.sciencemag.org/cgi/content/full/301/5629/105/DC1](http://www.sciencemag.org/cgi/content/full/301/5629/105/DC1)  
 Materials and Methods  
 Figs. S1 and S2

14 March 2003; accepted 30 May 2003

## Intracellular Bacterial Biofilm-Like Pods in Urinary Tract Infections

Gregory G. Anderson, Joseph J. Palermo, Joel D. Schilling, Robyn Roth, John Heuser and Scott J. Hultgren

*Science* **301** (5629), 105-107.  
DOI: 10.1126/science.1084550

ARTICLE TOOLS	<a href="http://science.sciencemag.org/content/301/5629/105">http://science.sciencemag.org/content/301/5629/105</a>
SUPPLEMENTARY MATERIALS	<a href="http://science.sciencemag.org/content/suppl/2003/07/02/301.5629.105.DC1">http://science.sciencemag.org/content/suppl/2003/07/02/301.5629.105.DC1</a>
RELATED CONTENT	<a href="http://science.sciencemag.org/content/sci/301/5629/31.1.full">http://science.sciencemag.org/content/sci/301/5629/31.1.full</a>
REFERENCES	This article cites 30 articles, 18 of which you can access for free <a href="http://science.sciencemag.org/content/301/5629/105#BIBL">http://science.sciencemag.org/content/301/5629/105#BIBL</a>
PERMISSIONS	<a href="http://www.sciencemag.org/help/reprints-and-permissions">http://www.sciencemag.org/help/reprints-and-permissions</a>

Use of this article is subject to the [Terms of Service](#)